Available online at www.sciencedirect.com
ScienceDirect
International Journal of Solids and Structures 44 (2007) 1423–1437
INTERNATIONAL JOURNAL OF SOLIDS and STRUCTURES
www.elsevier.com/locate/ijsolstr

Analysis of the failure mode and softening behaviour of sands in true triaxial tests

Wenxiong Huang *, De'an Sun, Scott W. Sloan

Discipline of Civil, Surveying and Environmental Engineering, University of Newcastle, Callaghan NSW 2308, Australia

Received 5 December 2005; received in revised form 12 June 2006
Available online 22 June 2006

Abstract

This paper presents a theoretical analysis and a numerical study of the failure mode in sands based on a hypoplastic description of the material. A bifurcation analysis is performed to study the failure mode in sands under true triaxial stress conditions at the material response level. It is shown that either uniform failure or localized failure can occur, depending on the intermediate principal stress. Uniform bifurcation occurs in tests along stress paths with a lower Lode angle, including the stress path for a conventional triaxial compression test. Localized failure occurs in tests along stress paths with a higher Lode angle, including stress paths for biaxial compression and triaxial extension tests. Specimen responses under laboratory conditions are then studied numerically by 3D FE simulations of biaxial compression, triaxial compression, and triaxial extension tests. The effects of initial imperfection from a homogeneous state are taken into account by introducing a frequency distribution of the initial void ratio. This permits the softening behaviour and shear localization in sand specimens to be analysed for different degrees of initial heterogeneity.

Keywords: Failure mode; Softening; Shear localization; Degree of heterogeneity

1. Introduction

It is well known that the shear strength of sand-like granular materials is governed by the confining pressure and strongly influenced by the density of the granular packing. Strain softening behaviour is widely observed in dense and medium-dense sands, and is usually accompanied by a volumetric dilation which arises because of the need to overcome grain interlocking during shear. Constitutive modelling of such behaviour often requires a density-related quantity as a state variable, which makes it possible to describe the complicated pressure- and density-dependent behaviour using a set of state-independent constitutive parameters (Been and Jefferies, 1985; Gudehus, 1996; Li and Dafalias, 2000).

* Corresponding author. Tel.: +61 2 4921 6082; fax: +61 2 4921 6991.
E-mail address: wenxiong.huang@newcastle.edu.au (W. Huang).

0020-7683/$ - see front matter
doi:10.1016/j.ijsolstr.2006.06.026

Calibrating softening behaviour in the laboratory is by no means trivial. Indeed, strain-controlled tests, such as triaxial tests or true triaxial tests, are required. Due to the possibility of bulging or non-uniform deformation of the specimen, the data obtained from an average stress–strain curve may not represent a real material response. To obtain a true material response, the specimen needs to undergo uniform deformation in the hardening phase, the peak state, and the softening phase. A cubical testing apparatus may be better for this purpose than a conventional triaxial test apparatus with a cylindrical specimen. Whatever test is used, it is crucial that the specimen has a homogeneous initial state, and that the loading plates are greased to minimize the influence of surface friction.

Even if these precautions are applied in a test, a uniform deformation pattern is not guaranteed throughout the loading range. Localized deformation in the form of shear bands is often observed in biaxial compression tests (e.g. Arthur et al., 1977; Vardoulakis, 1980; Finno et al., 1997; Mokni and Desrues, 1998) and triaxial extension tests (Reades and Green, 1976; Yamamuro and Lade, 1995), and is sometimes also noted in triaxial compression tests (Peters et al., 1988). In the following discussion, the term *failure* is used to refer to the state of a specimen at its maximum load bearing capacity, which corresponds to the apparent peak average stress observed in a test. Note that failure may occur under uniform deformation conditions or localized deformation conditions. The former is referred to as uniform peak failure and is indicated by a gradual degradation of the average strength after the peak is reached. The latter, termed localized failure, is characterized by the development of shear bands around the apparent peak and is often indicated by a sudden reduction in the average strength. Other types of failure may occur, such as bulging failure which is chiefly caused by friction on the top and bottom faces of a specimen acting in combination with a flexible lateral boundary, but these are not the concern of this study.

Based on an experimental study with sand in a true triaxial testing apparatus, Wang and Lade (2001) recently observed that localized failure or uniform peak failure can occur in medium dense to dense sands in true triaxial tests, depending on the stress path. The failure mode and the apparent peak strength are significantly affected by the intermediate principal stress. Defining the parameter $b = (\sigma_2 - \sigma_3)/(\sigma_1 - \sigma_3)$ to characterize the role of the intermediate principal stress σ_2, they concluded that, for tests with b falling in the range of 0.18–0.85, shear localization occurs in the hardening regime. For tests with a lower or higher value of b, shear banding can only occur in the softening regime.

We note that in the tests of Wang and Lade (2001), shear banding is identified by an abrupt change of slope in the average stress–strain and strain–strain curves, which is in fact an indirect observation. It is possible that some minor slope changes may be missed, or that some of the detected slight slope changes are a result of initial imperfections which might be avoidable in a test with a better prepared specimen.

This paper presents a theoretical analysis and a numerical study of the occurrence of shear localization and possible failure mode in sands under true triaxial stress conditions. A hypoplastic model (Gudehus, 1996; Bauer, 1996), which can capture many key features of sand-like granular materials with a single set of state-independent parameters, is employed for this study. The theoretical analysis is based on a bifurcation criterion for the hypoplastic continuum that tells the state during loading at which shear localization may occur (Huang et al., 2005). This criterion is used to predict the failure mode along various stress paths, its dependence on the intermediate-principal stress, and the influence of the initial pressure and density.

While the bifurcation analysis provides a valuable insight into the failure mode as an intrinsic material response, the structural response of a sand specimen may also be affected by initial imperfections and the boundary conditions. A 3-D finite element study is performed to simulate experimental conditions with cubical specimens. The inherent heterogeneity in specimens is taken into account by introducing a frequency distribution in the initial void ratio. Using the two-parameter frequency distribution of void ratio proposed by Bhatia and Soliman (1990), the effects of the degree of initial heterogeneity are studied by assigning different values for the deviation while keeping the same average value for the initial void ratio in the simulations.

It is well-known that grain size and grain rotation play an important role in the development of shear bands. These polar effects can be taken into account with a micropolar continuum model (e.g. Tejchman and Bauer, 1996; Huang et al., 2002). Numerous studies on polar effects in granular materials with the development of shear localization have been done. For example, Mühlhaus and Vardoulakis (1987), de Borst (1991), and Ehlers and Volk (1998) used an elastoplastic approach, while Tejchman and Gudehus (2001) and Huang and Bauer (2003) employed micropolar hypoplastic models. The present study is mainly concerned

with the emergence of shear localization, and it shown that this can be predicted successfully with a conventional continuum hypoplastic model.

This work is motivated by some earlier results of the second author, who conducted a series of modified true triaxial tests on sands with rigid boundaries. While the first author performed the numerical analyses, the work is a result of discussions among all three authors.

2. Constitutive description of the material

In this analysis, sand is described as a continuum obeying a hypoplastic constitutive law. This type of constitutive model defines a stress–strain relation using a single nonlinear tensor-valued function, and does not decompose the strain rate into elastic and plastic parts. A detailed description of the theory of hypoplasticity can be found in Kolymbas (2000). In this study, the hypoplastic model for sands formulated by Gudehus (1996) and Bauer (1996) is employed. It is assumed that the response of sand to loading is governed by the current stress $\boldsymbol{\sigma}$ and the void ratio e. The constitutive equations are given as

$$\begin{aligned} \dot{\boldsymbol{\sigma}} &= f_s[\hat{a}^2\dot{\boldsymbol{\varepsilon}} + \hat{\boldsymbol{\sigma}}(\hat{\boldsymbol{\sigma}} : \dot{\boldsymbol{\varepsilon}}) + f_d\hat{a}(\hat{\boldsymbol{\sigma}} + \hat{\boldsymbol{\sigma}}^d)||\dot{\boldsymbol{\varepsilon}}||], \\ \dot{e} &= (1+e)\mathrm{tr}\,\dot{\varepsilon}. \end{aligned} \tag{1}$$

Here the objective stress rate $\dot{\boldsymbol{\sigma}}$ is given as a nonlinear function of the strain rate $\dot{\boldsymbol{\varepsilon}} = \frac{1}{2}[\nabla\dot{\boldsymbol{u}} + (\nabla\dot{\boldsymbol{u}})^T]$ with $\nabla\dot{\boldsymbol{u}}$ being the velocity gradient, $||\dot{\boldsymbol{\varepsilon}}|| = \sqrt{\dot{\boldsymbol{\varepsilon}} : \dot{\boldsymbol{\varepsilon}}}$ being a Euclidean type norm of the strain rate, and $\hat{\boldsymbol{\sigma}} = \boldsymbol{\sigma}/\mathrm{tr}\,\boldsymbol{\sigma}$ being the normalized stress tensor with the deviator $\hat{\boldsymbol{\sigma}}^d = \hat{\boldsymbol{\sigma}} - 1/3$. The parameter $\hat{a}$ is related to the limit stress at the critical state, which is characterized by a simultaneous vanishing of the stress and volume changes for continuing deformation. The current model enforces a unit value for the factor f_d and the following condition on the stress as the critical state is approached (Bauer, 1996):

$$||\hat{\boldsymbol{\sigma}}^d|| = \hat{a}. \tag{2}$$

The SMP limit stress condition of Matsuoka and Nakai (1977) is incorporated in this model by taking the following expression for the parameter $\hat{a}$ (Bauer, 2000):

$$\hat{a} = \hat{a}_i\left(\sqrt{\frac{3}{8}||\hat{\boldsymbol{\sigma}}_d||^2 + \left(1 - \frac{3}{2}||\hat{\boldsymbol{\sigma}}_d||^2\right)\Big/\left(1 - \sqrt{\frac{3}{2}}||\hat{\boldsymbol{\sigma}}_d||\cos(3\theta)\right)} + \sqrt{\frac{3}{8}}||\hat{\boldsymbol{\sigma}}_d||\right), \tag{3}$$

where $\hat{a}_i$ is related to the critical state friction angle φ_c through

$$\hat{a}_i = \sqrt{\frac{8}{3}}\frac{\sin\varphi_c}{3 + \sin\varphi_c}. \tag{4}$$

The scalar factors f_s and f_d in Eq. (1) describe the pressure and density dependence of the material behaviour. They are functions of the mean pressure $p = -\mathrm{tr}\,\boldsymbol{\sigma}/3$ and the void ratio e according to $f_s = (1/\hat{\boldsymbol{\sigma}} : \hat{\boldsymbol{\sigma}})(e_i/e)^\beta(3p/h_s)^{1-n}f_b^*$ and $f_d = (r_e)^\alpha$, where f_b^* is a coefficient that can be determined from the consistency condition for isotropic compression and r_e is a relative void ratio defined as (Gudehus, 1996)

$$r_e = \frac{e - e_d}{e_c - e_d}. \tag{5}$$

The constants α and β scale the density-dependent peak state and tangential stiffness, while the quantities e_i, e_d and e_c represent the maximum, the minimum and the critical void ratio (which all vary with the pressure on the granular skeleton). The pressure-dependency of these quantities may be described by the following exponential relations (Bauer, 1996; Gudehus, 1996):

$$e_c/e_{c0} = e_d/e_{d0} = e_i/e_{i0} = \exp[-(3p/h_s)^n], \tag{6}$$

where e_{i0}, e_{d0} and e_{c0} are material constants corresponding to the loosest, the densest and the critical void ratios at a nearly stress-free state, and h_s and n ($0 < n < 1$) are two material constants used to fit the experimental data (Bauer, 1996).

Note that the density of a granular soil is conventionally defined using a relative density index $D_r = (e_{max} - e)/(e_{max} - e_{min})$, where e_{max} and e_{min} are determined from standard testing procedures. The relative void ratio r_e defined in (4) differs from D_r in the following aspects: (1) r_e is pressure dependent while D_r is not; (2) r_e decreases as the density increases, with $r_e = 1$ for $e = e_c$ and $r_e > 1$ for looser states; and (3) D_r is usually determined at a very low pressure state, with e_{max} being close to e_c and e_{min} usually being greater than e_d under the same stress conditions (Herle and Gudehus, 1999). Therefore r_e is usually somewhat greater than $1 - D_r$.

Shearing of medium dense to dense sand will lead to a peak state, followed by strain-softening before it reaches the critical state asymptote. Such behaviour is well-described by the present constitutive model with a relative smaller initial r_e value. At the peak state, stress changes vanish under a continuing dilatation so that $\dot{\boldsymbol{\sigma}} = 0,\ \dot{e} > 0$ and $f_d < 1$. This leads to the following condition that the stress and void ratio fulfill (Huang et al., 2005):

$$\psi_p(\hat{\boldsymbol{\sigma}}, e) = \frac{f_d^2}{\hat{a}^2}[\eta^2 ||\hat{\boldsymbol{\sigma}}||^2 + (2\eta + 1)||\hat{\boldsymbol{\sigma}}^d||^2] - 1 = 0, \tag{7}$$

where $\eta = (\hat{a}^2 - ||\hat{\boldsymbol{\sigma}}^d||^2)/(\hat{a}^2 + ||\hat{\boldsymbol{\sigma}}||^2)$. Note that the critical state, represented by (2), is independent of the initial density of the granular packing, while the peak state is dependent on the initial density.

3. Shear bifurcation in hypoplastic continuum

In a true triaxial test, a cubical specimen can be loaded independently in three orthogonal directions coinciding with the direction of the principal stress or the principal strain. This makes it possible to explore a large variety of stress paths without rotation of the principal stress and strain axes. The test results can be interpreted as a material response as long as the specimen maintains a uniform deformation.

Depending on the stress and density state, shear localization may occur in an initially homogeneous specimen. The possibility of shear bands emerging can be predicted from bifurcation analysis. Pioneered by Rudnicki and Rice (1975) and Rice (1976), the method assumes that a uniformly deforming specimen may reach an equilibrium state at which the relevant constitutive model allows non-uniform deformation to occur in the form of a planar weak discontinuity. The analysis does not take into account any length scale or the effect of the boundary conditions, so that the predicted shear bifurcation represents an intrinsic characteristic of the material under specified stress and density states. Bifurcation analysis can provide valuable insights into the occurrence of shear localization, but should be augmented by a study of the effects of the stress and density state and the boundary conditions. These factors have an important influence on the structural response of a deforming specimen and will be examined numerically later. Nevertheless, the bifurcation point on a stress path can be considered to be an upper limit for maintaining uniform deformation in a specimen.

Using the hypoplastic law described in the foregoing section, a bifurcation criterion has been derived by Huang et al. (2005). This follows the general procedure proposed by Chambon et al. (2000) for incrementally nonlinear constitutive models and is now briefly summarized.

Consider loading in an initially homogeneous and isotropic granular material that causes a uniform deformation with an increase in deviatoric stress and a change in the void ratio. The velocity and the stress fields are continuous up to a state at which planar weak discontinuities may develop. Across a weak discontinuity plane the velocity and stress fields are initially continuous, but the gradient of velocity will experience a jump which can be expressed as (Rice, 1976)

$$[\![\nabla \boldsymbol{v}]\!] = \boldsymbol{g} \otimes \boldsymbol{n}. \tag{8}$$

Here $[\![\nabla \boldsymbol{v}]\!]$ denotes the jump of a quantity across a weak discontinuity plane, $\boldsymbol{n}$ is a unit vector normal to the discontinuity plane, and $\boldsymbol{g}$ is a characteristic bifurcation vector which is non-trivial when a weak discontinuity occurs. A nonlinear equation for the bifurcation vector $\boldsymbol{g}$ can be obtained by ensuring that equilibrium is satisfied along the discontinuity plane and applying the constitutive relation

$$\boldsymbol{\Pi g} = \lambda f_d \boldsymbol{r}. \tag{9}$$

In this equation, the scalar factor $\lambda = [\![\sqrt{\dot{\boldsymbol{\varepsilon}} : \dot{\boldsymbol{\varepsilon}}}]\!]$, the vector $\boldsymbol{r} = -\hat{a}(\hat{\boldsymbol{\sigma}} + \hat{\boldsymbol{\sigma}}^d)\boldsymbol{n}$, and the coefficient tensor

$$\mathbf{\Pi} \approx (\hat{a}/2)[\mathbf{1} + \boldsymbol{n} \otimes \boldsymbol{n} + (\hat{\boldsymbol{\sigma}}\boldsymbol{n}) \otimes (\hat{\boldsymbol{\sigma}}\boldsymbol{n})] \tag{10}$$

are introduced, where $\mathbf{1}$ is a unit tensor of rank 2. Since $\mathbf{\Pi}$ is invertible (Huang et al., 2005), the existence of a solution for Eq. (9) is associated with a non-trivial solution for the factor λ, which is possible only when the following condition is met:

$$\psi_b(\hat{\boldsymbol{\sigma}}, e, \boldsymbol{n}) = \frac{1}{2} f_d^2 [\hat{\boldsymbol{g}} \cdot \hat{\boldsymbol{g}} + (\hat{\boldsymbol{g}} \cdot \boldsymbol{n})^2] - 1 \geqslant 0, \tag{11}$$

where the vector $\hat{\boldsymbol{g}} = \mathbf{\Pi}^{-1}\boldsymbol{r}$ is a function of the normalized stress $\hat{\boldsymbol{\sigma}}$ and the vector $\boldsymbol{n}$ only.

Inequality (11) is the bifurcation condition for the present hypoplastic continuum, and it must be fulfilled by the stresses and void ratio for shear bands to occur. The function $\psi_b(\hat{\boldsymbol{\sigma}}, e, \boldsymbol{n})$ has a negative value at an isotropic stress state and its value increases with the deviatoric stress during loading. The equality

$$\psi_b(\hat{\boldsymbol{\sigma}}, e, \boldsymbol{n}) = 0 \tag{12}$$

is used as the criterion to predict the onset of shear localization in a uniformly deforming granular material whose behaviour is described by the present hypoplastic model.

4. Prediction of failure modes in sand

In this section, the shear bifurcation condition (12) is used to predict the failure modes of sand specimens undergoing true triaxial testing. An initially isotropic stress state is assumed in a material element with a mean pressure represented by p_0 and a corresponding initial density represented by the relative void ratio r_{e0}. Strain-controlled tests along various stress paths are simulated with constant mean pressure. These stress paths are specified by a constant Lode angle or b-value in the deviatoric stress plane, where the Lode angle $\theta = \arctan[\sqrt{3}(\sigma_2 - \sigma_3)/(2\sigma_1 - \sigma_2 - \sigma_3)]$ is related to the parameter b through the expression

$$\tan\theta = \sqrt{3}b/(2 - b). \tag{13}$$

During loading, the stresses and void ratio are determined by integrating the constitutive equations. The constitutive parameters used in the study are those calibrated for Toyoura sand (Herle and Gudehus, 1999). Tests are simulated for the sand with an initial relative void ratio in the range of $0.1 < r_{e0} < 0.9$. The peak stress state and bifurcation state are identified by the conditions (7) and (12). For a material under the same initial mean pressure and relative void ratio, the peak stress state depends on the Lode angle and can be represented by a point on the stress path in a deviatoric stress plane. All the peak stress points form a conical surface in principal stress space which is open along the hydro-static axis and has a slightly curved generatrix. This peak stress surface can be represented by a closed curve in the normalized deviatoric plane at a given mean pressure. Fig. 1 presents the peak stress surface on the normalized deviatoric stress plane at a

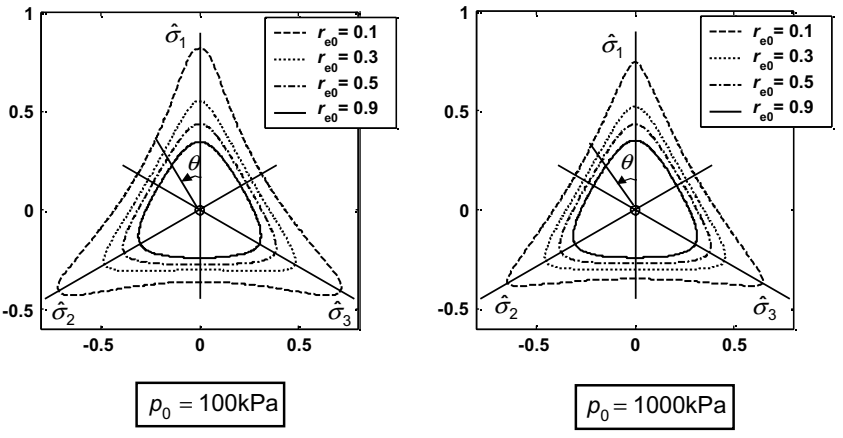

Fig. 1. Peak stress states represented in the normalized deviatoric stress plane.

mean pressure of $p_0 = 100$ kPa and $p_0 = 1000$ kPa, respectively. These peak stress surfaces are obtained for different initial densities with r_{e0} ranging from 0.1 to 0.9. As expected, these plots show that the peak stress surface expands as the initial density is increased. The rounded peak stress surface for the looser sands becomes more angular as the initial relative void ratio decreases.

If the bifurcation condition is met in the hardening regime, a localized failure is predicted. Otherwise, a uniform peak failure is indicated. The bifurcation condition may also be met in the softening regime after the peak. In this case, the softening behaviour observed in a laboratory test may be affected by shear localization.

Bifurcation points are presented and compared with the peak stress points in Fig. 2. The bifurcation point is found to coincide with the peak point for a Lode angle θ_1 of about 17–18°, which corresponds to a b value of approximately 0.3. This angle decreases slightly as the initial density decreases (r_{e0} increases). For stress paths with a Lode angle $|\theta| > \theta_1$, shear bifurcation occurs in the hardening regime before the peak, while for some stress paths with $|\theta| \in (\theta_0, \theta_1)$ bifurcation occurs in the softening regime after the peak. For stress paths with a Lode angle less than a critical value θ_0, which includes the stress path for triaxial compression ($\theta = 0$), bifurcation does not occur at all. This critical value of the Lode angle is influenced by the initial density, and increases rapidly with r_{e0} (decreasing initial density). For a very dense initial state with $r_{e0} = 0.1$ we have $\theta_0 \approx 2.5°$, while θ_0 varies from 13° to 14° for r_{e0} in the range 0.2–0.7.

The peak and bifurcation stress points are identified by fulfilment of the conditions (7) and (12), respectively, and are illustrated in Fig. 3. Fig. 3(a) and (b) shows a bifurcation point detected before the peak, Fig. 3(c) and (d) shows a bifurcation point detected after the peak, and Fig. 3(e) and (f) shows a case where no bifurcation point is detected at all. Bifurcation does not occur along the stress path in the last case as the function ψ_b has a maximum value which is less than 0.

Bifurcation in the hardening regime prior to the peak state indicates that failure occurs as banded shear localization. Uniform deformation at the peak state may be achieved in tests if there is no shear bifurcation or if the bifurcation develops after the peak. The results presented here predict that localized failure will occur in the hardening regime for stress paths with a Lode angle greater than $\theta_1 \approx 17°$. This includes stress paths for biaxial compression and triaxial extension. For stress paths with a Lode angle which is less than θ_0, including

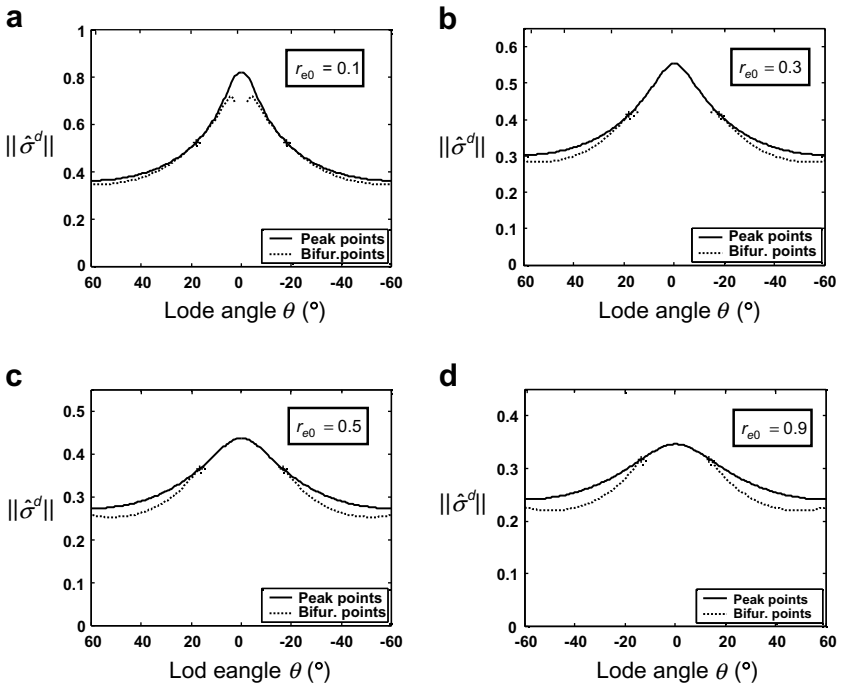

Fig. 2. Dependence of peak and bifurcation stress point with Lode angle: tests with initial mean pressure $p_0 = 100$ kPa and density index of (a) $r_{e0} = 0.1$, (b) $r_{e0} = 0.3$, (c) $r_{e0} = 0.5$ and (d) $r_{e0} = 0.9$.

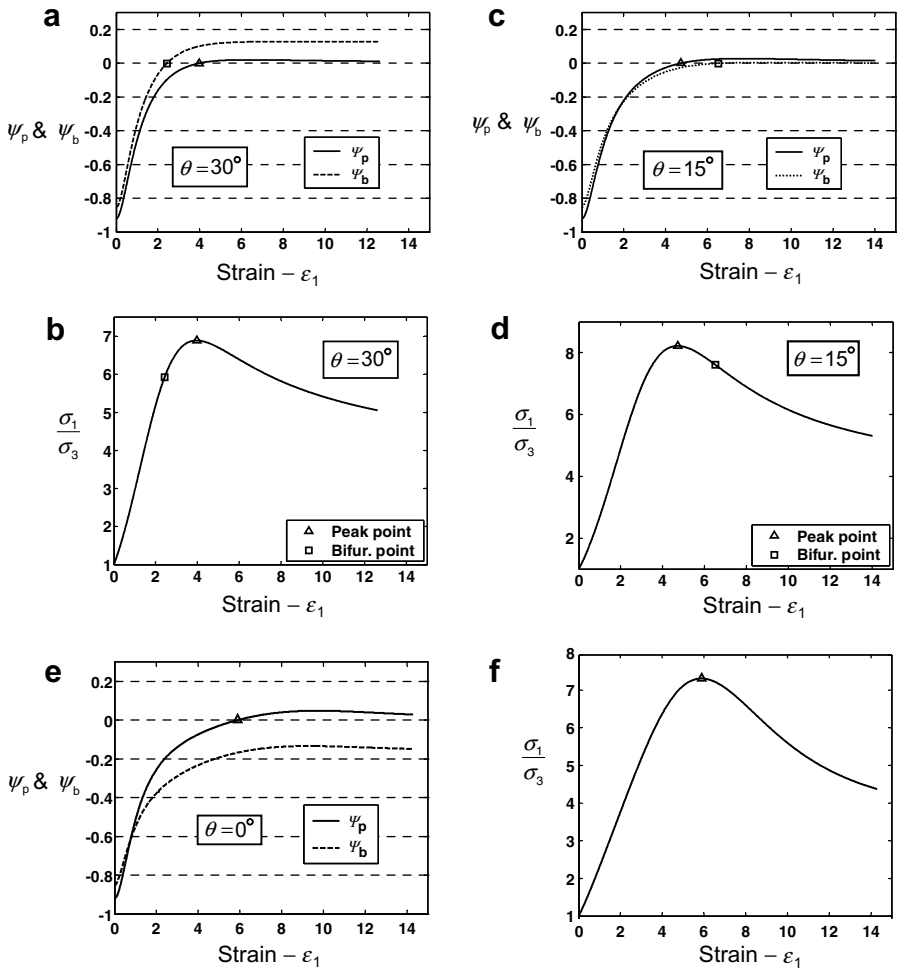

Fig. 3. Determination of bifurcation point ($p_0 = 100$ kPa, $r_{e0} = 0.3$): (a) and (b) bifurcation before peak stress for stress path with $\theta = 30°$, (c) and (d) bifurcation after the peak stress for stress path with $\theta = 15°$, (e) and (f) no bifurcation along the stress path with $\theta = 0°$.

the stress path for triaxial compression, bifurcation is not predicted and a peak failure with uniform deformation is suggested. For stress paths where $\theta_0 < |\theta| < \theta_1$, a uniform peak state may be followed by shear localization. These results are generally consistent with the experimental observations of Wang and Lade (2001). However, Wang and Lade's results suggest that shear localization may also occur in the softening regime of triaxial compression tests after a certain amount of post peak straining (see also Lade, 2003). This discrepancy may due to the inability of the model to predict real material behaviour. However, it may also be caused by some unidentified factors that are affecting the experimental results.

In determining the bifurcation point, the maximum value of the function ψ_b is found by searching over all possible orientations for a weak discontinuity plane which is characterized by the vector n. At those bifurcation points, it is found that the discontinuity plane emerges with its normal vector n perpendicular to the intermediate principal stress, i.e., a shear band often occurs in a plane which is perpendicular to the plane of the intermediate principal stress. The orientation of this shear plane is therefore fully defined by the angle ϕ between the normal to the shear plane and the maximum principal stress direction as sketched in Fig. 4(a). The predicted angle ϕ varies with the initial density of the granular material and the Lode angle as shown in Fig. 4(b). It increases as the initial relative void ratio r_{e0} decreases. This is in consistency with the experimental observations (Lade and Wang, 2001). For a given initial relative void ratio, the predicted maximum inclination angle is obtained at a Lode angle of $\theta = \theta_1$, which corresponds to the stress path along which

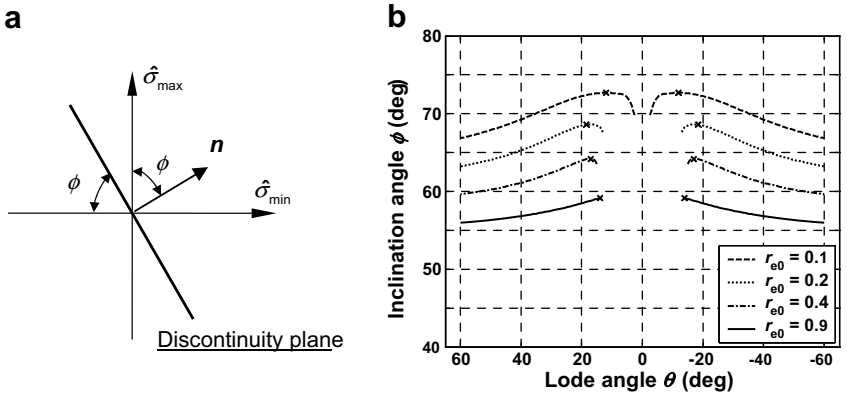

Fig. 4. Inclination of weak discontinuity plane with respect to the principal stress directions.

the bifurcation point coincides with the peak point. The further the bifurcation point is away from the peak point, the smaller the predicted inclination angle is. This tendency is also exhibited in the experimental data. The discrepancy that the predicted shear band inclination decreases with an increased Lode angle for $\theta > \theta_1$ is associated to the inaccuracy of the peak stress state predicted by the constitutive model. As the Matsuoka–Nakai criterion is incorporated in the current constitutive model, improvement may be expected by incorporating the Lade criterion (Lade, 1977). Compared with the former, the Lade criterion, which predicts a slightly higher peak friction angle for $\theta > 0$, especially for θ close to 60°, is better supported by the experimental data (Lade, 2006).

5. Modelling of initial heterogeneity in sand specimens

The bifurcation analysis in the foregoing section predicts the possible failure modes as a material response in true triaxial tests. Laboratory tests, however, also incorporate a structural response of the specimen which is dependent on the boundary conditions and any initial imperfections. A prepared sand specimen can never be ideally homogeneous on the micro-level, and the stress tensor fluctuates from point to point in a macroscopically homogeneous specimen. The void ratio varies from one 'Voronoi cell' to another (Shahinpoor, 1981), and lies between a minimum value of e_m and a maximum value of e_M. Even in a granular packing of equal-sized spheres, the void ratio shows a frequency distribution (Shahinpoor, 1981, 1982). This inherent heterogeneity at the micro-level may initiate strain localization in a specimen under loading, even though a uniform peak failure is predicted from bifurcation analysis.

In finite element simulations of sand tests, the effects of initial heterogeneity may be taken into account by introducing a random distribution of the initial void ratio which is permitted to vary from the mean value. Nübel and Karcher (1998) performed a numerical study of shear localization in sand by using an exponential frequency distribution for the initial void ratio proposed by Shahinpoor (1981)

$$f(e) = \frac{\lambda \exp(-\lambda e)}{\exp(-\lambda e_m) - \exp(-\lambda e_M)}. \tag{14}$$

They demonstrated that realistic shear localization patterns can be obtained in a granular body with such a frequency distribution. Nübel (2002) also showed that a random fluctuation in the stress distribution can be initiated by adopting a frequency distribution in the void ratio.

We note that Shahinpoor's frequency distribution stems from the theory of statistical mechanics and experiments using equal-sized hard spheres. It contains only one parameter λ, which is uniquely determined by the mean void ratio $\bar{e}$. This means that two granular packings with the same mean void ratio have exactly the same frequency distribution. However, for sands, it is possible that two specimens with the same mean void ratio have different void ratio deviations, and hence different frequency distributions. Bhatia and Soliman (1990) found, from their experiments with granular materials of different grain characters, that only sphere-grained

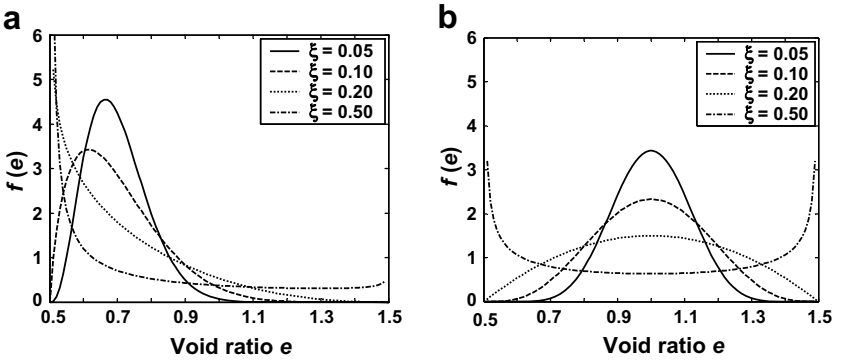

Fig. 5. Frequency distribution of void ratio for (a) $\bar{e} = 0.7$ and (b) $\bar{e} = 1.0$, with $e_m = 0.5$, $e_M = 1.5$.

materials (such as glass beads) have a frequency distribution that can be approximated by Eq. (14). For materials with angular particles, including sands, the frequency distribution of the void ratio is better represented by a β-distribution

$$f(e) = \frac{1}{B(p,q)} \frac{(e-e_m)^{p-1}(e_M-e)^{q-1}}{(e_M-e_m)^{p+q-1}}, \tag{15}$$

where $B(p,q)$ is the beta function. In this study, we adopt a β-distribution for the initial void ratio and determine the parameters p (>0) and q (>0) from the mean void ratio $\bar{e}$ and the mean square-root deviation s according to

$$p = \frac{\bar{e}-e_m}{e_M-e_m}\left(\frac{(\bar{e}-e_m)(e_M-\bar{e})}{s}-1\right), \quad q = \frac{e_M-\bar{e}}{e_M-e_m}\left(\frac{(\bar{e}-e_m)(e_M-\bar{e})}{s}-1\right). \tag{16}$$

To ensure a positive value for p and q, the deviation s is restricted to $s < (\bar{e}-e_m)(e_M-\bar{e})$. Furthermore, a parameter $\xi = s/(\bar{e}-e_m)(e_M-\bar{e})$ is introduced to characterize the degree of heterogeneity of the granular packing ($0 < \xi < 1$). Examples of the void ratio distribution, for a given mean void ratio and a varied deviation, are shown in Fig. 5. For smaller values of ξ, the frequency of the void ratio distribution is concentrated close to the mean void ratio and the material is therefore relatively homogeneous. Conversely, larger values of ξ lead to more heterogeneous materials. Indeed, these examples illustrate that a deviator of $\xi > 0.2$ implies a rather heterogeneous void ratio distribution, and a well-prepared sand specimen should typically have a void ratio frequency distribution with $\xi \leqslant 0.1$.

For a given granular packing, the minimum void ratio e_m and the maximum void ratio e_M bound the densest void ratio e_d and the loosest void ratio e_i on the macro scale. As a first estimation, $e_m \approx e_d$ may be assumed. According to Shahinpoor (1981), the critical state corresponds to a uniform frequency distribution $f_{cr} = 1$, that is, $e_c = \int_{e_m}^{e_M} f_{cr} e \, de = (e_m + e_M)/2$. Thus e_M can be estimated from

$$e_M \approx 2e_c - e_d. \tag{17}$$

To generate a numerical frequency distribution for the void ratio which obeys (14), a random number generator can be used to obtain random numbers of uniform deviation in $[0,1]$. Then a transformation method (Press et al., 1992) can be used with a transformation function $F^{-1}(y)$ which is the inverse of the function

$$F(y) = \frac{1}{B(p,q)} \int_0^y x^{p-1}(1-x)^{q-1} \, dx, \tag{18}$$

where x is related to the void ratio via $x = (e-e_m)/(e_M-e_m)$.

6. Numerical simulation of some basic tests

The specimen response is now studied by simulating laboratory tests using the three-dimensional nonlinear finite element program ABAQUS. A cubical specimen with dimensions 10 cm × 10 cm × 10 cm is assumed and

displacement-controlled biaxial compression (under plane strain conditions), triaxial compression, and triaxial extension tests are simulated with variations in the initial void ratio as described in the foregoing section. The hypoplastic constitutive model described earlier in the paper is implemented through the user subroutine interface. In simulating triaxial compression tests, pressure is applied to both lateral surfaces but their normal displacements are tied so as to model a rigid boundary. Under biaxial compression, the normal displacements (strains) on one of the lateral faces are prescribed to zero. In both cases, loading is applied by axial displacement (strain) control on the top surface. In the triaxial extension tests, a constant normal pressure is applied to both lateral surfaces with loading being applied by axial extension displacement control. In all these tests, an initial isotropic stress state with $p_0 = 98$ kPa is prescribed. The mean value for the initial void ratio is set at $\bar{e}_0 = 0.678$, which represents a dense sand with $r_{e0} = 0.35$. Initial heterogeneity is quantified by assigning different values for the deviation parameter ξ. The same constitutive parameters for Toyoura sand (Herle and Gudehus, 1999) are employed for all the numerical simulations.

The stress path for a biaxial compression test has a varying Lode angle, starting from about 12° at a nearly isotropic state to about 30° near the bifurcation point. Shear bifurcation in the hardening regime, prior to reaching the peak state, is predicted by the bifurcation analysis. Results from the numerical simulations are shown in Fig. 6. These are for tests with the initial heterogeneity quantified by $\xi_0 = 0.05$ and 0.3, representing a low degree and a high degree of initial heterogeneity, respectively. Two planar shear zones are clearly visible in the void ratio contour plots, with the lighter colour representing a higher void ratio or a looser state. These results suggest that shear localization can develop in biaxial compression, even when the initial void ratio is relatively uniform. The average stress ratios in the specimen, obtained by averaging the values of the stress components in the elements across a section, are plotted against the average strains in Fig. 6(f). Also shown on this plot is the stress ratio-strain curve from direct integration of the constitutive equation, which represents the material response without localization. The square symbol on this curve represents the theoretically predicted bifurcation point. The onset of shear localization in the numerical simulations, which is indicated by the contour plot of the deviatoric strain increment (Fig. 6(e)), is observed just prior to the peak of the average stress–strain curve. These results show that shear localization leads to a sharp drop in the average stress ratio. The average peak stress is less than the theoretical peak value because shear localization occurs prior to reaching this state under uniform deformation. The curves in Fig. 6(f) indicate that a stronger initial heterogeneity in the specimen leads to a slightly higher average peak stress. Interestingly, the rigid boundaries did not prevent shear localization from developing in the specimen. This has also been observed in experiments by Lade and Wang (2002) and Nübel (2002). Lade and Wang have also pointed out that the proximity of the smooth end plates influences the onset of shear banding. This effect is not considered here as an ideally smooth rigid-boundary is assumed in the finite element simulations.

In contrast to biaxial compression, the bifurcation analysis for triaxial compression predicts that the peak failure strength will be reached under uniform deformation conditions and that no bifurcation will occur over the whole loading range. To check this prediction various finite element simulations of a triaxial compression test were performed, taking into account the influence of initial heterogeneity. Contour plots of the void ratio and the deviatoric strain indicated that no shear bands were developed in any of the simulations, even with a strong initial heterogeneity $\xi_0 = 0.3$. Indeed, the void ratio plots shown in Fig. 7 suggest that loading decreases the density variation, so that the specimen becomes less heterogeneous. It should be noted, however, that for specimens with a high degree of initial heterogeneity (reflected by a large value of ξ_0) numerical difficulties were encountered in the finite element computations. These difficulties were characterized by the solution failing to converge in a reasonable number of equilibrium iterations, and occurred after the peak strength was reached. This behaviour may suggest the development of a stronger type of non-uniformity and may finally lead to some form of shear localization in the softening regime as observed (Wang and Lade, 2001) but, nevertheless, uniform peak failure was observed. For the specimen with a low initial heterogeneity ($\xi_0 = 0.05$), the average stress–strain curve is almost the same as that for the material response (Fig. 7(e)). The softening behaviour from such a test can, therefore, be considered as a material response and the results can be used to calibrate constitutive models. The curves in Fig. 7(e) also show that a higher degree of initial heterogeneity leads to a higher average peak stress ratio.

For triaxial extension, the theoretical analysis predicts that shear bifurcation will occur in the hardening regime at a point which is close to the peak state (refer to Fig. 2). Wang and Lade (2001), however, observed

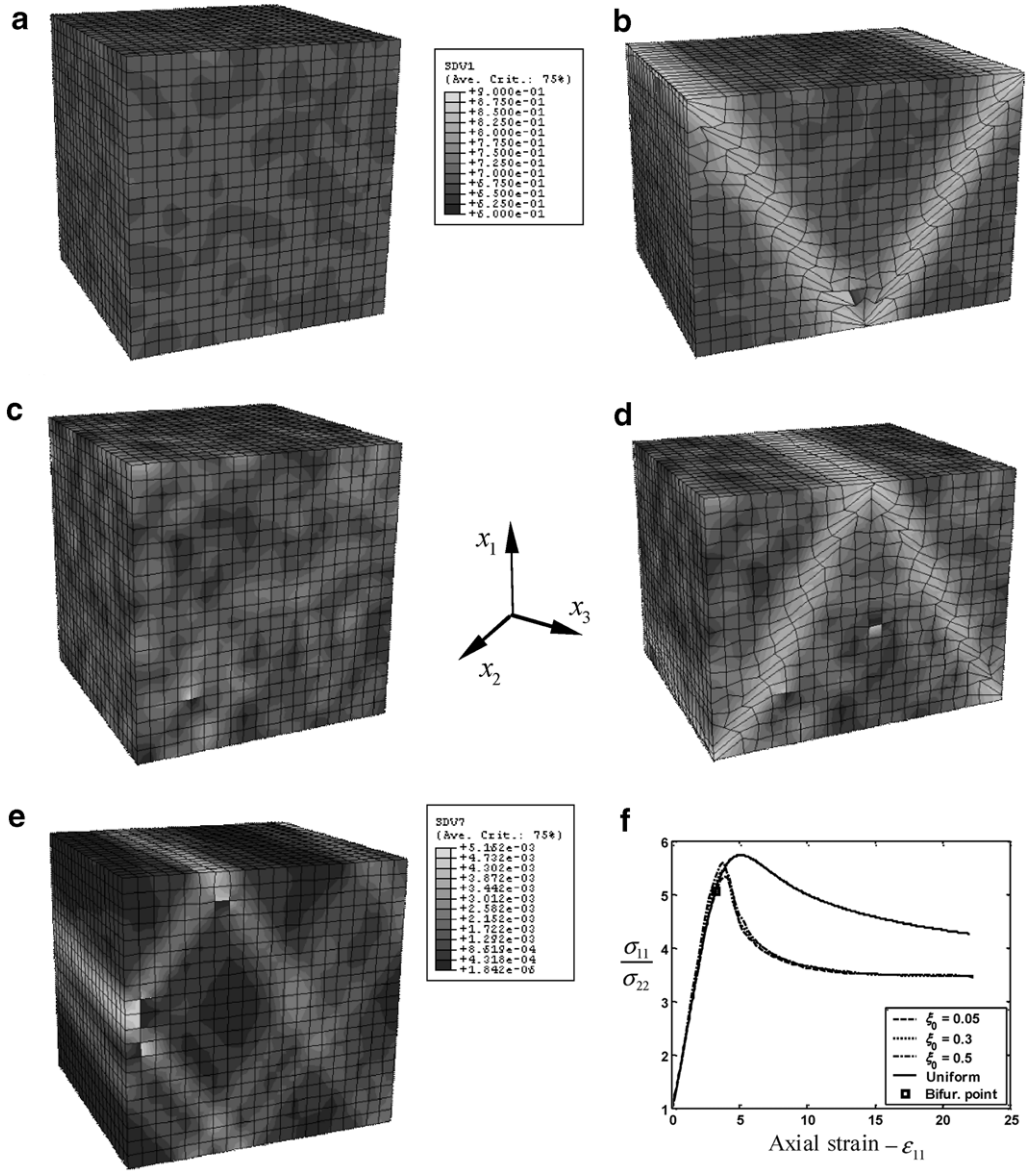

Fig. 6. Numerical simulation of biaxial compression tests: contour plot of (a) initial and (b) final void ratio for $\xi_0 = 0.05$, (c) initial and (d) final void ratio for $\xi_0 = 0.3$, (e) deviatoric strain increment just prior the peak ($\xi_0 = 0.05$), and (f) average stress–strain curves.

shear banding in the post-peak softening regime, where the onset of shear banding was identified by a sudden change in the gradient of the stress–strain or strain–strain curve. While bifurcation analysis predicts the response of a material element, experimental results are affected by the testing conditions, the boundary conditions, and the initial state. Yamamuro and Lade (1995) noted that the conventional triaxial extension test is inherently unstable. Some requirements, such as enforcement of a uniform strain in the specimen, need to be applied to measure a proper material response.

Numerical results from finite element simulations of specimen tests are presented in Fig. 8. The influence of the initial heterogeneity of a sand specimen is again considered by assuming a varied heterogeneity in the frequency distribution of the initial void ratio. Shear bands are observed in all these tests, as shown in the contour plots (Fig. 8(b) and (d)) for specimens with an initial heterogeneity of $\xi_0 = 0.05$ and $\xi_0 = 0.3$, respectively. Again, we detected the onset of shear localization from contour plots of the deviatoric strain increment, as

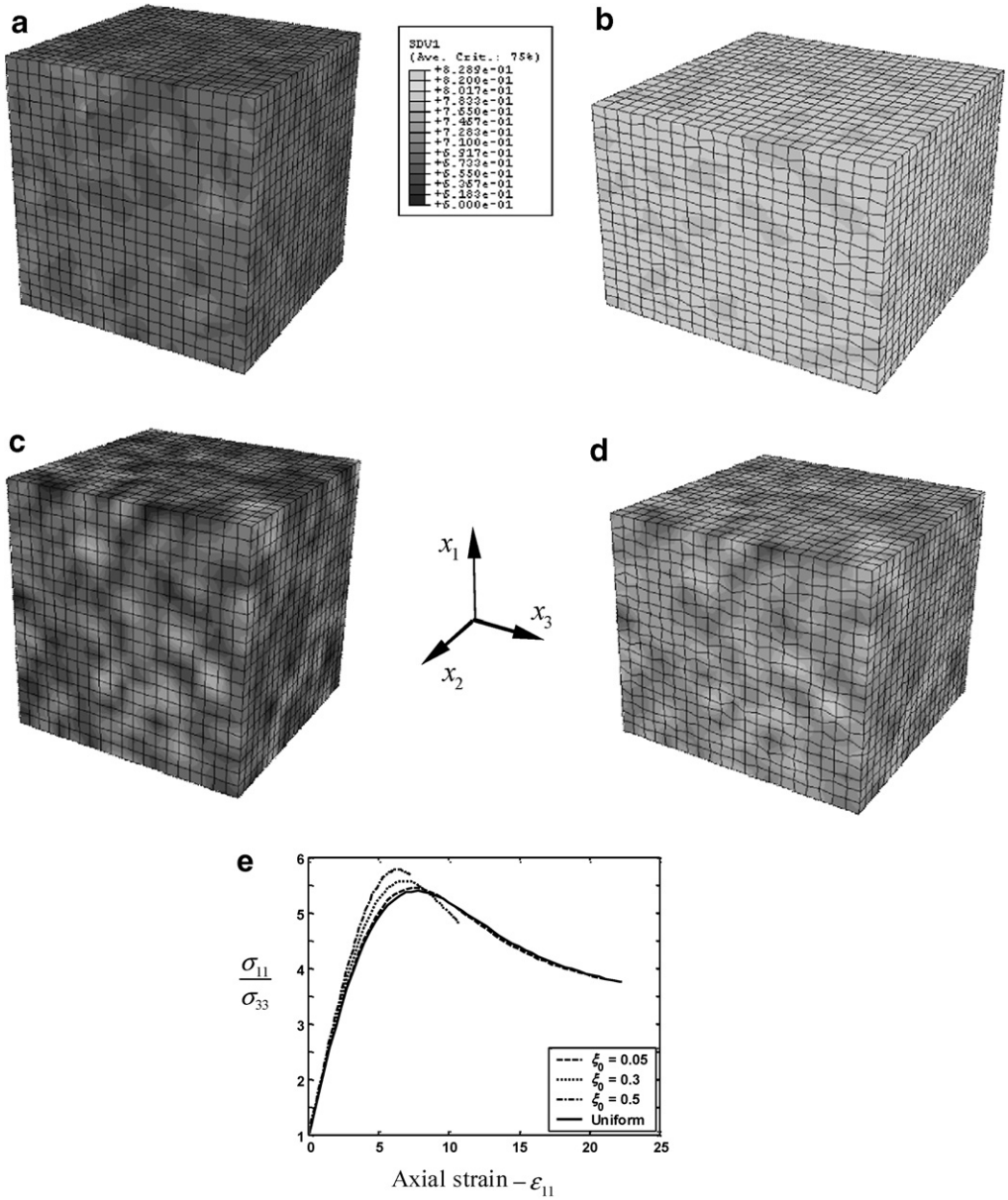

Fig. 7. Numerical simulation of triaxial compression tests: contour plot of (a) initial and (b) final void ratio for $\xi_0 = 0.05$, (c) initial and (d) final void ratio for $\xi_0 = 0.3$; (e) average stress–strain curves.

displayed in Fig. 8(e). For the test with a strong initial heterogeneity ($\xi_0 = 0.3$), shear localization starts to develop around the peak state. For the relatively homogeneous specimen ($\xi_0 = 0.05$), however, the onset of shear banding occurs in the post-peak softening regime. This is in accordance with the experimental observations of Wang and Lade (2001). In all these numerical simulations, the onset of shear localization is detected at a larger strain than that predicted from bifurcation analysis, which is marked by a square symbol in Fig. 8(f). The corresponding average stress–strain curve indicates uniform deformation at the peak strength, but the softening is much stronger compared with the response obtained from direct integration of the constitutive model. Compared with the bifurcation analysis prediction, the onset of shear localization is delayed. Results from numerical simulations of triaxial extension tests are somewhat sensitive to the initial conditions.

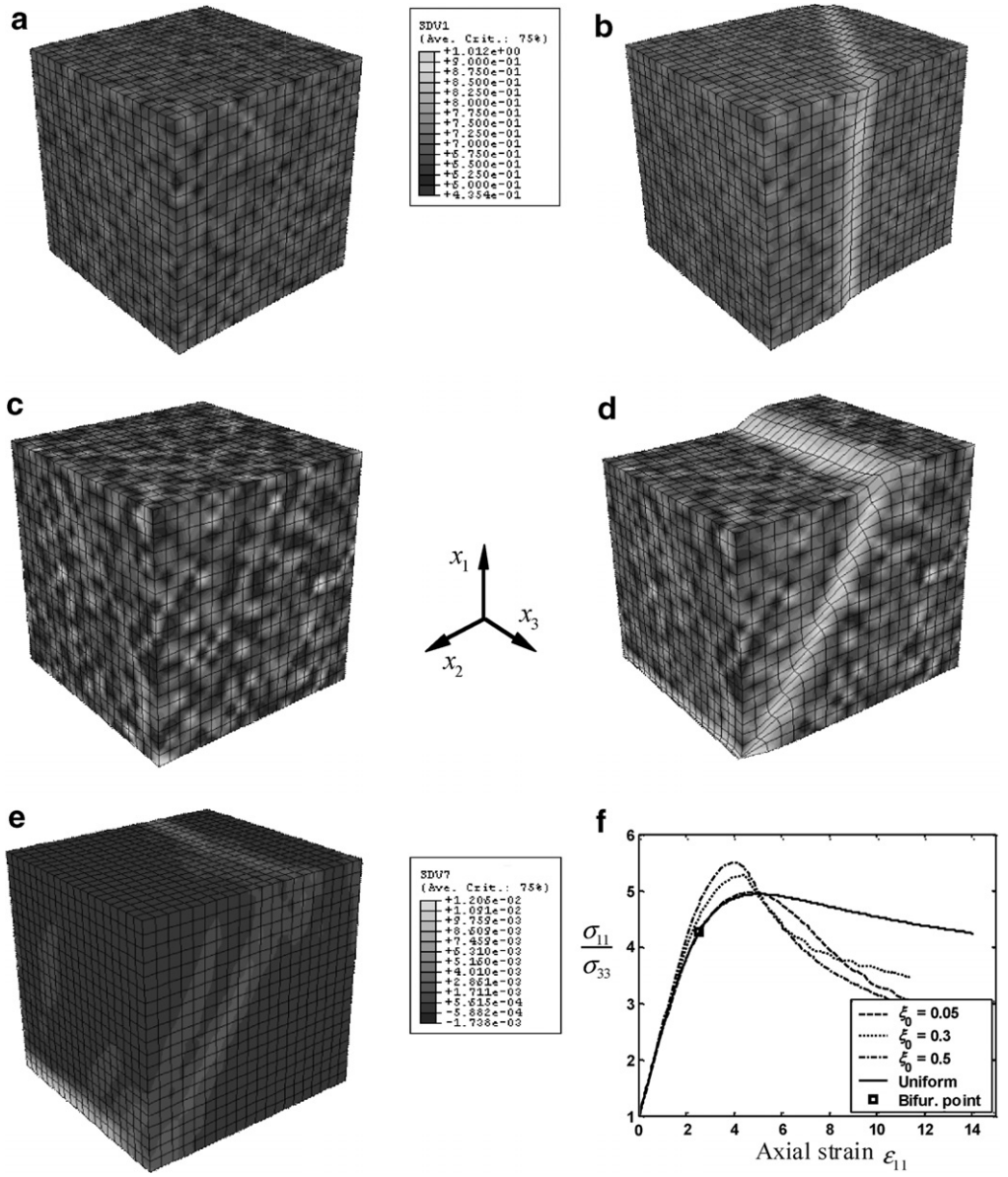

Fig. 8. Numerical simulation of triaxial extension tests: contour plot of (a) initial and (b) final void ratio for test with $\xi_0 = 0.05$, (c) initial and (d) final void ratio for test with $\xi_0 = 0.3$, (e) deviatoric strain increment around peak for test with $\xi_0 = 0.3$; (f) average stress–strain curves.

7. Conclusions

Based on a bifurcation analysis, three-dimensional finite element simulations and a hypoplastic constitutive law, the failure mode in medium dense to dense sands under true triaxial test conditions has been studied. The bifurcation theory predicts that the failure mode is dependent on the intermediate principal stress (or the Lode angle). Moreover, it is predicted that shear bifurcation occurs in the pre-peak hardening regime for stress paths with a Lode angle greater than a critical value of about 17°. For stress paths with a Lode angle less that this critical value, bifurcation can occur in the post-peak softening regime. Shear bifurcation is not predicted at all in tests following stress paths with a very low Lode angle. In the deviatoric stress plane, this zone of no-bifurcation is evenly bisected by the stress path for triaxial compression.

The structural responses of specimens under biaxial compression, triaxial compression and triaxial extension conditions have been studied numerically. The influence of initial imperfections on the failure mode and softening behaviour in specimens has been examined. The finite element simulations suggest that initial imperfections do not change the failure mode in biaxial compression tests or triaxial compression tests. In biaxial compression, the deformation was strongly localized in banded shear zones prior to reaching the peak strength. The average stress–strain curves exhibited a softening which was much stronger than that predicted by the material response obtained from direct integration of the hypoplastic constitutive law. In the triaxial extension simulations, shear localization developed either around the peak state or in the post-peak softening regime, and this was found to be affected by the degree of initial heterogeneity. The onset of shear localization occurs at a strain greater than that at which bifurcation is theoretically predicted. Initial imperfections increased the apparent peak strength slightly and amplified the rate of softening. Although uniform peak failure can be obtained in triaxial compression tests, the post-peak softening behaviour can be influenced by the type of test, the initial heterogeneity of the specimen, and the boundary conditions. Localized bifurcation can occur in various ways in conventional cylindrical or cubical triaxial compression tests. However, the present work showed that the true material response may be obtained from a well-conducted cubical triaxial compression test. It follows that the experimental results so obtained can be used to calibrate constitutive models.

Acknowledgement

The financial support of Australia Research Council (Grant DP0453056) is acknowledged by the first author.

References

Arthur, J.R.F., Dunstan, T., Al-Ani, Q.A.J.L., Assadi, A., 1977. Plastic deformation and failure in granular media. Géotechnique 27 (1), 53–74.

Bauer, E., 1996. Calibration of a comprehensive hypoplastic model for granular materials. Soils Foundations 36 (1), 13–26.

Bauer, E., 2000. Conditions for embedding Casagrade's critical state into hypoplasticity. Mech. Cohesive-Frict. Mater. 5 (2), 125–148.

Been, K., Jefferies, M.G., 1985. A state parameter for sands. Géotechnique 35 (1), 99–112.

Bhatia, S.K., Soliman, A.F., 1990. Frequency distribution of void ratio of granular materials determined by an image analyzer. Soils Foundations 30 (1), 1–16.

Chambon, R., Crochepeyer, S., Desrues, J., 2000. Localization criteria for non-linear constitutive equations of geomaterials. Mech. Cohesive-Fric. Mater. 5 (1), 61–82.

de Borst, R., 1991. Simulation of strain localisation: a reappraisal of the Cosserat continuum. Eng. Comput. 8, 317–332.

Ehlers, W., Volk, W., 1998. On theoretical and numerical methods in the theory of porous media based on polar and non-polar elasto-plastic solid materials. Int. J. Solids Struct. 35 (34–35), 4597–4617.

Finno, R.J., Harris, W.W., Mooney, M.A., Viggiani, G., 1997. Shear bands in plane strain compression of loose sand. Géotechnique 47 (1), 149–165.

Gudehus, G., 1996. A comprehensive constitutive equation for granular materials. Soils Foundations 36 (1), 1–12.

Herle, I., Gudehus, G., 1999. Determination of parameters of a hypoplastic constitutive model from properties of grain assemblies. Mech. Cohesive-Fric. Mater. 4 (5), 461–486.

Huang, W., Bauer, E., 2003. Numerical investigations of shear localization in a micro-polar hypoplastic material. Int. J. Numer. Anal. Meth. Geomech. 27 (4), 325–352.

Huang, W., Nübel, K., Bauer, E., 2002. Polar extension of a hypoplastic model for granular materials with shear localization. Mech. Mater. 34 (9), 563–576.

Huang, W., Hjiaj, M., Sloan, S.W., 2005. Bifurcation analysis for shear localization in non-polar and micro-polar hypoplastic continua. J. Eng. Math. 52, 167–184.

Kolymbas, D., 2000. Introduction to Hypoplasticity. A.A. Balkema, Rotterdam.

Lade, P.V., 1977. Elasto-plastic stress–strain theory for cohesionless soils with curved yield surface. Int. J. Solids Struct. 13 (11), 1019–1035.

Lade, P.V., 2003. Analysis and prediction of shear banding under 3D conditions in granular materials. Soils Foundations 43 (4), 161–172.

Lade, P.V., 2006. Assessment of test data for selection of 3-D failure criterion for sand. Int. J. Numer. Anal. Meth. Geomech. 30 (3), 307–333.

Lade, P.V., Wang, Q., 2001. Analysis of shear banding in true triaxial tests on sand. J. Eng. Mech., ASCE 127 (8), 762–768.

Lade, P.V., Wang, Q., 2002. Effect of slenderness ratio on shear banding in true triaxial tests on sand. In: Pande, G.N., Pietruszczak, S. (Eds.), Proc. of the 8th Int. Symp. On Numerical Model in Geomechanics – NUMOG VIII. A.A. Balkema, pp. 149–154.

Li, X.S., Dafalias, Y.F., 2000. Dilatancy for cohesionless soils. Géotechnique 50 (4), 449–460.

Matsuoka, H., Nakai, T., 1977. Stress–strain relationship of soil based on the 'SMP'. In: Proc. 9th Int. conf. Soil Mech. Found. Eng., Tokyo, pp. 153–162.
Mokni, M., Desrues, J., 1998. Strain localization measurements in undrained plane-strain biaxial tests on Hostun RF sand. Mech. Cohesive-Frict. Mater. 4, 419–441.
Mühlhaus, H.-B., Vardoulakis, I., 1987. The thickness of shear bands in granular materials. Géotechnique 37 (3), 271–283.
Nübel, K., 2002. Experimental and numerical investigation of shear localization in granular materials. Veröffentlichungen des Institutes für Bodenmechanik und Felsmechanik der Universität Fridericiana in Karlsruhe, Heft 159.
Nübel, K., Karcher, C., 1998. FE simulations of granular material with a given frequency distribution of voids as initial condition. Granular Matter 1, 105–112.
Peters, J.F., Lade, P.V., Bro, A., 1988. Shear band formation in triaxial and plane strain tests. In: Donaghe, R.T. et al. (Eds.), Advanced Triaxial Testing of Soil and Rock, ASTM STP 977, Philadelphia.
Press, W.H., Teukolsky, S.A., Vetterling, W.T., Flannery, B.P., 1992. Numerical Recipes in Fortran 77 – The Art of Scientific Computing, second ed. The University of Cambridge Press.
Reades, D.W., Green, G.E., 1976. Independent stress control and triaxial extension tests on sand. Géotechnique 26 (4), 551–576.
Rice, J.R., 1976. The localization of plastic deformation. In: Koiter, W.T. (Ed.), Theoretical and Applied Mechanics. North-Holland Publishing Company, pp. 207–220.
Rudnicki, J.W., Rice, J.R., 1975. Conditions for the localization of deformation in pressure-sensitive dilatant materials. J. Mech. Phys. Solids 23 (6), 371–394.
Shahinpoor, M., 1981. Statistical mechanical considerations on storing bulk solids. Bulk Solids Handling 1 (1), 31–36.
Shahinpoor, M., 1982. Frequency distribution of voids in monolayers of randomly packed equal spheres. Bulk Solids Handling 2 (4), 825–837.
Tejchman, J., Bauer, E., 1996. Numerical simulation of shear band formation with a polar hypoplastic constitutive model. Compt. Geotech. 19 (3), 221–244.
Tejchman, J., Gudehus, G., 2001. Shearing of a narrow granular layer with polar quantities. Int. J. Numer. Anal. Meth. Geomech. 25, 1–28.
Vardoulakis, I., 1980. Shear band inclination and shear modulus of sand in biaxial tests. Int. J. Numer. Anal. Meth. Geomech. 4, 103–119.
Wang, Q., Lade, P.V., 2001. Shear banding in true triaxial tests and its effect on failure in sand. J. Eng. Mech., ASCE 127 (8), 754–761.
Yamamuro, J.A., Lade, P.V., 1995. Strain localization in extension tests on granular materials. J. Eng. Mech., ASCE 121 (7), 828–836.